Biogeosciences
Discussions

Open Access

EGU

1

2 **Ammonia impacts methane oxidation and methanotrophic community in**

3 **freshwater sediment**

4

5 Yuyin Yang[1], Jianfei Chen[1], Shuguang Xie[1,*], Yong Liu[2]

6

7 [1]State Key Joint Laboratory of Environmental Simulation and Pollution Control,

8 College of Environmental Sciences and Engineering, Peking University, Beijing

9 100871, China

10

11 [2]Key Laboratory of Water and Sediment Sciences (Ministry of Education), College of

12 Environmental Sciences and Engineering, Peking University, Beijing 100871, China

13

14

15 * Corresponding author. Tel: 86-10-62751923. Email: xiesg@pku.edu.cn (S Xie)

16

17

18

19

20

21

Biogeosciences Open Access

Discussions

EGU

22   **Abstract**

23   Lacustrine ecosystems are an important natural source of greenhouse gas methane.

24   Aerobic methanotrophs are regarded as a major regulator controlling methane

25   emission. Excess nutrient input can greatly influence carbon cycle in lacustrine

26   ecosystems. Ammonium is believed to be a major influential factor, due to its

27   competition with methane as the substrate for aerobic methanotrophs. To date, the

28   impact of ammonia on aerobic methanotrophs remains unclear. In the present study,

29   microcosms with freshwater lake sediment were constructed to investigate the

30   influence of ammonia concentration on aerobic methanotrophs. Ammonia influence

31   on the abundance of *pmoA* gene was only observed at a very high ammonia

32   concentration, while the number of *pmoA* transcripts was increased by the addition of

33   ammonium. *pmoA* gene and transcripts differed greatly in their abundance, diversity

34   and community compositions. *pmoA* transcripts were more sensitive to ammonium

35   amendment than *pmoA* gene. Methane oxidation potential and methanotrophic

36   community could be impacted by ammonium amendment. This work could add some

37   new sights towards the links between ammonia and methane oxidation in freshwater

38   sediment.

39

42

Biogeosciences
Open Access
EGU
Discussions

43

1. Introduction

44

45 Methane is a major product of carbon metabolism in freshwater lakes, and also a

46 critical greenhouse gas in the atmosphere (Bastviken et al., 2004). Aerobic methane

47 oxidation performed by bacterial methanotrophs is a major pathway controlling

48 methane emission. Up to 30–99% of the total methane produced in anoxic sediment

49 can be oxidized by methanotrophs (Bastviken et al., 2008). Methane oxidation in

50 freshwater lakes can be greatly influenced by the environmental changes (e.g.

51 eutrophication) induced by anthropogenic activities (Borrel et al., 2011).

52

53 The increasing input of nutrients into freshwater lakes has greatly raised the

54 availability of dissolved organic carbon (DOC), nitrogen and phosphorus, and also

55 exerted a considerable influence on aerobic methane oxidation (Liikanen and

56 Martikainen, 2003; Veraart et al., 2015). Among various types of nutrients, ammonia

57 has attracted great attention. Ammonium and methane have similar chemical

58 structure, and ammonium is known to compete with methane for the binding site of

59 methane monooxygenase, a key enzyme in methane oxidation (Bédard and Knowles,

60 1989). On the other hand, a high concentration of oxygen in lake water might also

61 inhibit methane oxidation (Rudd and Hamilton, 1975), and excess ammonia can lead

62 to the competition between methane oxidizers and ammonium oxidizers for oxygen.

63 With high oxygen availability or low in-situ nitrogen content, methane oxidation can

Biogeosciences
Open Access
Discussions
EGU

64   also be stimulated by the addition of ammonium (Rudd et al., 1976). Hence, the effect

65   of ammonium on methane oxidation is complex (Bodelier and Laanbroek, 2004), and

66   previous studies have documented contradictory results, such as inhibition (Bosse et

67   al., 1993; Murase and Sugimoto, 2005; Nold et al., 1999), no effect (Liikanen and

68   Martikainen, 2003), or stimulation (Bodelier et al., 2000; Rudd et al., 1976). The

69   effect of ammonium on methane oxidation might largely depend on the characteristics

70   of the studied ecosystem and in-situ environment (Bodelier and Laanbroek, 2004;

71   Borrel et al., 2011).

72

73   To date, previous studies about the ammonium effect on methane oxidation in

74   freshwater lakes mainly focused on either oxidation rate or net methane flux (Bosse et

75   al., 1993; Liikanen and Martikainen, 2003; Murase and Sugimoto, 2005). However,

76   methanotrophs play a fundamental role in regulating methane emission from

77   freshwater sediment (Bastviken et al., 2008). The abundance, transcription, and

78   community structure of aerobic methanotrophs may also be affected by the extra input

79   of ammonium (Shrestha et al., 2010). The difference in methanotrophic community

80   structure can further lead to various responses of methane oxidation to nitrogen

81   content (Jang et al., 2011; Mohanty et al., 2006; Nyerges and Stein, 2009). Therefore,

82   identification of the variation of methanotrophic community can be helpful to

83   understand how ammonium input influences methane oxidation process. The

84   community change of methanotrophs under ammonium stress has been observed in

Biogeosciences
Discussions

Open Access

EGU

85   various soils, such as agriculture soil (Seghers et al., 2003; Shrestha et al., 2010) and

86   landfill soil (Zhang et al., 2014). The results of these previous studies suggested that

87   the effect of ammonium on methanotroph community might be habitat-related. A

88   recent filed work suggested that in-situ ammonia concentration might be a key

89   regulating factor of methanotrophic community structure in freshwater lake sediment

90   (Yang et al., 2016). However, the direct evidence for the influence of ammonium (or

91   ammonia) on methanotroph community in freshwater lake sediment is still lacking.

92   Hence, in the present study, microcosms with freshwater lake sediment were

93   constructed to investigate the ammonium influence on methane oxidation potential

94   and the abundance, transcription and community structure of aerobic methanotrophs.

95

96   **2． Materials and methods**

97   *2.1. Sediment characteristics*

98   Dianchi Lake is a large shallow lake (total surface area: 309 km^2; average water

99   depth: 4.4 m) located in southeast China (Yang et al., 2016). This freshwater lake is

100   suffering from anthropogenically-accelerated eutrophication (Huang et al., 2017).

101   Surface sediment (0–5 cm) (24.9286N, 102.6582E) were collected using a core

102   sampler from the north part of Dianchi Lake in October, 2017. In-situ dissolved

103   oxygen (DO) and ammonium nitrogen (NH_4^+-N) in overlying water were 8.37 mg/L

104   and 344 μM, respectively. Sediment total organic carbon (TOC), total nitrogen (TN),

105   the ratio of TOC to TN (C/N), nitrate nitrogen (NO_3^--N), ammonium nitrogen (NH_4^+-

106 N), total phosphorus (TP), and pH were 41.3 g/kg, 3.95 g/kg, 10.5, 12.3 mg/kg, 364

107 mg/kg, 0.60 g/kg, and 7.2, respectively. Sediment (2 L) was transported to laboratory

108 at 4ºC for incubation experiment.

109

110 *2.2. Experimental setup*

111 Sediments were placed at room temperature for 24 h and then homogenized. The

112 homogenized sediments were centrifuged at 5000 rpm for 10 min to determine the

113 initial ammonia concentration of pore water. A series of 50-mL serum bottles (as

114 microcosms) were added with 10 mL of sediment aliquot (containing about 0.1 g dry

115 sediment). A total of 111 microcosms were constructed, including three autoclaved

116 ones used as the control for the measurement of methane oxidation potential. Six

117 treatments (A–F) were set up. The microcosms with treatments B–F were added with

118 1 mL of NH_4Cl at the levels of 5, 20, 50, 100, and 200 mM, respectively, while the

119 microcosm with treatment A was amended with 1 mL diluted water as the blank

120 control. For each treatment, 18 microcosms were constructed, including half used for

121 molecular analyses and another half for methanotrophic potential measurement. These

122 microcosms were closed with butyl rubber stoppers and incubated for 14 days at 25ºC

123 at 100 rpm in dark.

124

125 At each sampling time point (day 1 (12 h after incubation), day 7 or day 14), triplicate

126 sediment samples of each treatment were transferred into Falcon tubes, and then

127 centrifuged at 5000 rpm for 10 min. The supernatant was filtered with a 0.2-μm

128 syringe filter, and its ammonia level was measured using Nessler reagent-colorimetry.

129 The sediment was mixed up and immediately used for nucleic acid extraction. In

130 addition, at each sampling time, for methanotrophic potential measurement, another

131 three bottles of each treatment were opened and shaken to provide ambient air, then

132 closed again with butyl rubber stoppers. Headspace air (1 mL) was replaced by CH_4

133 (99.99%) with an air-tight syringe. Samples were shaken vigorously to mix. After

134 incubation at 25ºC, 100 rpm for 24 h, 0.1 mL of headspace gas was taken and

135 measured using a GC126 gas chromatograph equipped with a flame ionization

136 detector. Autoclaved control was also processed to exclude methane loss due to

137 dissolution or airtightness.

138

139 *2.3. Nucleic acid extraction, reverse transcription and quantification*

140 Sediment DNA and RNA were extracted with PowerSoil DNA Isolation Kit (MoBio)

141 and PowerSoil Total RNA Isolation Kit (MoBio, USA), respectively. The quality and

142 concentration of extracted nucleic acids were examined with Nanodrop 2000 (Thermo

143 Fisher Scientific, USA). RNA was diluted to a similar concentration before further

144 analysis. Real-time PCR of *pmoA* gene was performed on a CFX Connect cycler

145 (Bio-Rad, USA), using the primer set A189f/mb661r following the conditions

146 reported in our previous study (Liu et al., 2015). Reactions were carried out using a

147 TransStart Top Green qPCR Kit (Transgen, China) following the manufacturer's

148   instructions. Gene transcripts were quantified in a one-step RT-qPCR using a

149   TransScript Green One-step qRT-PCR Kit. Melting curve analyses were carried out at

150   the end of PCR run to check the amplification specificity. Each measurement was

151   carried out with three technical replicates. Standard curve was constructed with *pmoA*

152   gene clones, and the efficiency and r-square were 91.5% and 0.998, respectively.

153

154   *2.4. Terminal restriction fragment length polymorphism (T-RFLP) fingerprinting*

155   DNA *pmoA* gene fragment was amplified with primer sets A189f/mb661r, with the

156   forward primer A189f modified with FAM at 5'-end. PCR reactions were performed

157   as previously described (Liu et al., 2015). Two-step RT-PCR was carried out on

158   RNA. In the first step, RNA was reversely transcribed into cDNA with *pmoA* gene

159   specific primer using One-step gDNA removal and cDNA synthesis kit (Transgen

160   Biotech Co., LTD, China). The 20-μL reaction solution contained 1 μL EasyScript

161   RT/RI Enzyme Mix, 1 μL gDNA remover, 10 μL 2×ES Reaction Mix, 2 pmol of gene

162   specific primers and 1 μL RNA template. The reaction mixture was incubated at 42ºC

163   for 30 min, and the enzymes were deactivated at 85ºC for 5 s. In the second step, 1 μL

164   cDNA was used as template in *pmoA* gene PCR amplification, proceeded following

165   the same protocol with DNA.

166

167   The fluorescently labeled PCR products were purified using a TIANquick Mini

168   Purification Kit (TIANGEN Bitotech Co., Ltd, China). Approximately 20 ng of

169   purified PCR products were digested with restriction endonuclease *BciT130* I (Takara

170   Bio Inc., Japan) following the conditions recommended by the manufacturer's

171   instruction. Electrophoresis of digested amplicons was carried out by Sangon Biotech

172   (China) using an ABI 3730 DNA analyzer (Thermo Fisher Scientific, USA). The

173   length of T-RFs was determined by comparing with internal standard using the

174   GeneScan software. Terminal restriction fragments (T-RFs) with similar length (less

175   than 2 bp difference) were merged, and T-RFs shorter than 50 base pairs (bp) or

176   longer than 508 bp were removed from the dataset. Relative abundance of each

177   fragment equaled to the ratio of its peak area to the total area. Minor T-RFs with

178   relative abundance less than 0.5 % were excluded for further analysis. The Shannon

179   diversity indices of *pmoA* gene and transcripts were calculated based on DNA and

180   RNA T-RFs, respectively.

181

182   *2.5. Cloning, sequencing and phylogenetic analysis*

183   *pmoA* gene clone library was generated with mixed DNA PCR products using a TA

184   cloning kit (TransGen Biotech Co., LTD, China). Randomly picked clones were

185   subjected to sequencing. The in silico cut sites of these *pmoA* sequences were

186   predicted using the online software Restriction Mapper

187   (http://www.restrictionmapper.org). The sequences of each T-RF, together with their

188   reference sequences from the GenBank database, were used for phylogenetic analysis.

189   A neighbor-joining tree was conducted with MEGA 7 (Kumar et al., 2016), and

Biogeosciences
Discussions

190   bootstrap with 1000 replicates was carried out to check the consistency. The

191   phylogenetic tree was visualized using iTOL v4.2 (Letunic and Bork, 2016). The

192   sequences used in phylogenetic analysis were deposited in GenBank database, and the

193   accessions were shown in Fig. 3.

194

195   *2.6. Statistical analysis*

196   Two-way ANOVA (analysis of variance) was carried out to determine the effect of

197   ammonia concentration and incubation time on CH_4 oxidation potential, gene

198   abundance and transcription. One-way ANOVA followed by Student-Newman-Keuls

199   test was adopted to detect the difference among treatments. The analysis was carried

200   out in *R*, using *R* packages stats (version 3.4.4) and agricolae (version 1.2-8).

201   Moreover, the comparison of methanotrophic communities in different microcosms,

202   using Redundancy Analysis (RDA) and clustering analysis, was carried out with *R*

203   package Vegan (version 2.4-6) (Oksanen et al., 2018). Permutation test was carried

204   out to detect the margin effect of variables (treatment and time). Clustering analysis

205   was carried out based on Bray-Curtis dissimilarity, to demonstrate the variation of

206   microbial community structure during incubation.

207

208   **3. Results**

209   *3.1. Methane oxidation potential*

210   Ammonium was found to quickly deplete in each ammonium added microcosm (Fig.

211   S1). Methane oxidation potential (MOP) varied from 0.77 (in the microcosm with

212   treatment F on day 1) to 1.94 (in the microcosm with treatment F on day 14) mmol/g

213   dry sediment day (Fig. 1), while autoclaved control did not show notable methane

214   oxidation (data not shown). Based on two-way ANOVA, both ammonium

215   concentration (treatment) and incubation time had significant effects on MOP ($P<$

216   0.01), and their interaction was also significant ($P< 0.05$). The MOP in the microcosm

217   with treatment A (with no external ammonium addition) did not show a significant

218   difference among incubation times ($P>0.05$). Based on post-hoc test (Fig. 1, Table

219   S1), at each time, the microcosm with treatment B had slightly higher MOP than the

220   microcosm with treatment A. At days 1 and 7, the microcosms with treatments C, D

221   and E had slightly lower MOP than the un-amended microcosm. However, at each

222   time, no statistical difference in MOP was observed among the microcosms with

223   treatments A–E. Moreover, the microcosm with treatment F (with the highest

224   ammonium addition) tended to have significantly lower MOP than other microcosms

225   on day 1 ($P< 0.05$), but significantly higher MOP on day 14 ($P< 0.05$). On day 7, no

226   statistical difference in MOP was found between the microcosm with treatment F and

227   any other microcosms.

228

229   *3.2. pmoA gene and transcript abundance*

11

230   Two-way ANOVA indicated that the number of both *pmoA* gene and transcripts was

231   significantly influenced by ammonium concentration and incubation time ($P< 0.01$)

232   (Fig. 2a and 2b). The abundance of *pmoA* gene in the microcosm with treatment A

233   showed no significant difference among times ($0.05 < P < 0.1$). On day 1, the

234   microcosms with treatments C and D had higher (but not significantly) *pmoA* gene

235   abundance than other microcosms. However, at days 7 and 14, the microcosm with

236   treatment F (with the highest ammonium addition) had the highest *pmoA* gene

237   abundance.

238

239   At each time, *pmoA* transcripts in the un-amended microcosm was less abundant than

240   those in amended microcosms. On day 1, the highest number of transcripts was

241   observed in the microcosm with treatment C, followed by the microcosms with

242   treatments D, E and F. The microcosm with treatment B had much lower *pmoA*

243   transcript abundance than other ammonium added microcosms ($P< 0.05$) (Table S1).

244   On day 7, *pmoA* transcript abundance tended to increase with the level of added

245   ammonium, although statistical difference in *pmoA* transcript abundance was only

246   observed between treatment F and other treatments. On day 14, no significant

247   difference in *pmoA* transcript abundance was detected among treatments ($P> 0.05$).

248

249   The ratio of transcripts to *pmoA* gene varied with ammonium concentration and

250   incubation time (Fig. S2). The ratio tended to decrease with time in ammonium

12

Biogeosciences

Open Access

Discussions

EGU

251   amended microcosms. Moreover, at days 1 and 7, the ratio tended to increase with the

252   increasing ammonium concentration.

253

254   *3.3. T-RFLP fingerprinting*

255   In silico analysis of the cloned *pmoA* sequences showed that restriction enzyme

256   *BciT130* I could well capture *pmoA* gene diversity and present a good resolution

257   among different subgroups of aerobic methanotrophs. Most of the T-RFs retrieved in

258   the current study could be assigned to certain methanotrophic groups, while some of

259   the T-RFs from *pmoA* transcripts could not match the cut site predicted from the

260   sequences in clone library. The obtained *pmoA* sequences could be grouped into four

261   clusters (Fig. 3), which could be convincingly affiliated with known methanotrophic

262   organisms. Three clusters were affiliated with Type I methanotrophs

263   (*Gammaproteobacteria*), which could be further divided into several subgroups.

264   Cluster 1 contained 157 bp, 242 bp and 338 bp T-RFs that could be related to Type Ia

265   methanotrophs, the most frequently detected methanotrophs in freshwater lakes

266   (Borrel et al., 2011). The 157 bp and 338 bp T-RFs might be affiliated with

267   *Methylobacter* and *Methylomicrobium*, respectively. However, the 242 bp T-RF could

268   not be convincingly assigned to a certain genus because of the highly similar *pmoA*

269   sequences of Type Ia organisms. Cluster 2 was composed of three different T-RFs,

270   and could be affiliated with *Methylococcus* and *Methyloparacoccus*. Cluster 3

271   included the T-RFs of 91 bp and 508 bp, which might be closely related to

272 *Candidatus Methylospira*. Both cluster 2 and cluster 3 could be affiliated with Type

273 Ib methanotrophs, but they distinctly differed in phylogeny and morphology

274 (Danilova et al., 2016). Cluster 4 comprised of the T-RFs of 217 bp, 370 bp and 403

275 bp, and it was phylogenetically related to Type IIa methanotrophs (*Methylocystaceae*

276 in *Alphaproteobacteria*). The 403 bp T-RF was likely affiliated with *Methylosinus*,

277 while 217 bp and 370 bp T-RFs could not be convincingly assigned to a single genus.

278

279 The 508 bp fragment could be affiliated with either *Methylospira* or unknown Type Ia

280 methanotroph. Considering the low abundance of 508 bp T-RF (<0.5% in DNA

281 TRFLP profile and approximately 2% in RNA TRFLP profile), and in order to avoid

282 incorrect annotation, this T-RF was excluded from further analysis.

283

284 *3.4. T-RFLP diversity and profiles of pmoA gene and transcripts*

285 Diversity of each community was calculated based on T-RFLP results. In the current

286 study, the T-RFs with relative abundance more than 5% in at least one sample or with

287 average relative abundance more than 2% in all samples were defined as major T-

288 RFs. For a given sample, the total number of T-RFs and the number of major T-RFs

289 were greater in RNA T-RFLP profile than in DNA T-RFLP profile. On day 1,

290 ammonium amended microcosms tended to have lower *pmoA* gene diversity than un-

291 amended microcosm, while an opposite trend was found at days 7 and 14 (Table 1).

292 For a given sample, *pmoA* transcript showed higher Shannon diversity than *pmoA*

293   gene. Ammonium amended microcosms tended to have lower *pmoA* transcript

294   diversity than un-amended microcosm. In the microcosms with treatments A–D,

295   *pmoA* transcript diversity tended to increase with time. However, the Shannon

296   diversity of transcriptional T-RFs experienced an increase followed by a decrease in

297   the microcosms with treatments E and F.

298

299   A total of 11–14 T-RFs were retrieved from T-RFLP analysis of DNA samples. Most

300   of them (including all major T-RFs) could be well assigned to certain methanotrophic

301   groups (Figs. 3 and 4a). In all DNA samples, Type Ia and Type IIa methanotrophs

302   dominated methanotrophic communities. On day 1, the 242 bp T-RF (*Methylobacter-*

303   related Type Ia methanotrophs) comprised about 50% of methanotrophic

304   communities. The 370 bp T-RF (Type IIa methanotrophs) also showed a considerable

305   proportion (20–25%). The addition of ammonium tended to induce no considerable

306   change of methanotrophic community structure after 12-hour incubation. After 7 and

307   14 days of incubation, the proportions of major T-RFs illustrated an evident variation.

308   The proportion of Type Ia methanotrophs (157 bp, 242 bp and 338 bp; marked in

309   green) decreased with time, while Type IIa methanotrophs (217 bp and 370 bp,

310   marked in pink) increased. The proportion of *Methylococcus*-related Type Ib

311   methanotrophs (marked in blue) also increased, especially the 145 bp T-RF, whereas

312   the proportion of *Methylospira*-related Type Ib methanotrophs (91 bp, marked in

313   yellow) did not show a notable variation.

314

315   A total of 14–38 T-RFs were retrieved from T-RFLP analysis of RNA samples, but

316   most of them were only detected in a few samples with low relative abundance (Fig.

317   4b). Among the major transcript T-RFs, only 4 transcript T-RFs could be assigned to

318   a known methanotrophic group, and on day 1 they comprised of a considerable part of

319   methanotrophic community in un-amended microcosm (43–72%) and of in amended

320   microcosms (22–72%), while the other 7 T-RFs were not found in *pmoA* gene library

321   as well as DNA T-RFLP profiles. Compared with *pmoA* gene, the community

322   structure of *pmoA* transcripts was more sensitive to external ammonium addition. The

323   addition of ammonium induced a marked shift in *pmoA* transcriptional community

324   structure after 12-h incubation. The proportion of 242 bp increased, but the proportion

325   of 91 bp decreased. After 1 or 2 weeks' incubation, the microcosms with treatments

326   B, C, D and E had similar transcriptional community structure as the un-amended

327   microcosm. However, the microcosm with treatment F (with the highest ammonium

328   addition) encountered a remarkable increase in 91 bp (Ca. *Methylospira*-related Type

329   Ib methanotrophs). Moreover, the 370 bp T-RF, accounting for up to one fourth

330   (average) of DNA T-RFs, was only detected on day 14, with relative abundance of

331   0.8–2.9%.

332

333   *3.5. Clustering and statistical analysis of TRFLP profiles*

334   DNA- and RNA-based methanotrophic community structures were characterized with

335   hierarchal clustering based on Bray-Curtis dissimilarity (Fig. 5). *pmoA* community

336   structure was quite stable during the whole incubation period. Most of the samples on

337   day 1 were grouped together. Samples B7, D7, E7, B14, C14, D14, E14 and F14 were

338   clustered into another group. Sample D1 was distantly separated from other samples,

339

340   Higher dissimilarity of transcriptional community structures could be observed among

341   samples. The samples on day 1 were still close to each other, and they were clearly

342   separated from the samples at day 7 and 14. Samples A7, A14, B7, B14, D7, E7 and

343   F7 could form a clade, while samples C7, D14 and E14 formed another clade.

344   Moreover, sample F14 was distantly separated from other samples.

345

346   RDA with permutation test was carried out to test the potential relationship between

347   each major T-RF and factors (treatment and incubation time). The result indicated that

348   incubation time had a significant impact on DNA-based methantrophic community

349   composition ($P < 0.01$), while ammonium concentration did not exert a significant

350   influence ($P > 0.05$). The constrained variables could explain up to 74.4 % of total

351   variance. However, most of the explained variance (73.7% out of 74.4%) was related

352   to constrained axis 1, and only the first axis was significant ($P = 0.029$). In addition,

353   for RNA-based methantrophic community, treatment and time were able to explain

354   76.0% of total variance. Only incubation time had a significant effect on RNA-based

355   methantrophic community composition ($P < 0.01$), and only the first constrained axis

356   was significant ($P < 0.01$). These results indicated that after the addition and with the

357   depletion of ammonium, the community compositions of both *pmoA* gene and

358   transcripts could undergo a considerable shift.

359

360   **4.   Discussion**

361   *4.1.   Effect of ammonium on MOP*

362   The current study showed that a high dosage of ammonium could present a temporary

363   inhibition effect on methane oxidation. The result was consistent with several

364   previous studies (Bosse et al., 1993; Murase and Sugimoto, 2005; Nold et al., 1999).

365   These studies indicated that the addition of ammonium might inhibit methane

366   oxidation in water and sediment of freshwater lake. However, to date, the minimal

367   inhibit concentration for methane oxidation in lake sediment is still unclear. Bosse et

368   al. (1993) pointed out that methane oxidation in littoral sediment of Lake Constance

369   could be partially inhibited when ammonium concentration in pore water was higher

370   than 4 mM. In contrast, methane oxidation in sediment of hyper-eutrophic Lake

371   Kevätön was not obviously affected by a continuous water flow containing up to 15

372   mM of ammonium (Liikanen and Martikainen, 2003). Lake Kevätön and Dianchi

373   Lake had similar average water depth, and the overlying water of sediment in both

374   lakes had very high levels of ammonium (Liikanen and Martikainen, 2003). In the

375   present study, inhibition was only observed in the microcosm with a very high

376   ammonium dosage (with 17.3 mM ammonium in overlying water on day 1), while no

377   evident inhibition was found in the other ammonium amended microcosms, even at

378   high dosages. This suggested that methane oxidation might depend on ammonium

379   dosage, which was sustained by the result of two-way ANOVA. The minimal inhibit

380   concentration for methane oxidation in Dianchi Lake was much higher than that in

381   Lake Constance (Bosse et al. 1993). Hence, the minimal inhibition concentration for

382   methane oxidation could be lake-specific.

383

384   Despite of a very high dosage of ammonium, sediment MOP was only partially

385   inhibited. This might be explained by two facts. The studied sediment sample

386   originated from a eutrophic lake, which suffered from high ammonium input.

387   Methanotrophs in this kind of ecosystem could effectively oxidize methane under the

388   condition of high ammonia concentration (Liikanen and Martikainen, 2003). This was

389   consistent with the above-mentioned lake-related minimal inhibition concentration for

390   methane oxidation. On the other hand, the affinity of pMMO (*pmoA* encoding

391   protein) to methane is much higher than that to ammonium (Bédard and Knowles,

392   1989). As a result, when the methane concentration is high enough, as a common case

393   for the measurement of MOP, methanotrophs should be able to consume a

394   considerable amount of methane.

395

Biogeosciences
Discussions

Open Access

EGU

396   A recovery of MOP after a single-shot fertilization has been reported in forest soil

397   (Borjesson and Nohrstedt, 2000). In this study, it was noted that after the depletion of

398   ammonium, sediment MOP could also get a quick recovery. The highest ammonium

399   dosage eventually stimulated sediment MOP in the long run (about two weeks).

400   Considering the increase of *pmoA* gene abundance and the change of RNA-based

401   methantrophic community structure, this might be attributed to an adaption to the

402   environment. The initial decrease of MOP could be explained by the competition

403   between methane and ammonium for pMMO (Bédard and Knowles, 1989), while the

404   subsequent increase of MOP might be the consequence of the shift in methantrophic

405   community structure (Seghers et al., 2003; Shrestha et al., 2010) and the increase of

406   *pmoA* gene abundance and transcription.

407

408   *4.2. Effect of ammonium on pmoA gene and transcript abundance*

409   So far, little is known about the changes of methanotrophic abundance and transcripts

410   induced by external ammonium amendment. Alam and Jia (2012) reported that the

411   addition of 200 μg of nitrogen/g dry weight soil (in ammonium sulfate) showed no

412   significant influence on *pmoA* gene abundance in paddy soil. However, in

413   ammonium-amended rhizospheric soil microcosms, *pmoA* gene abundance slightly

414   increased after 29 days' incubation (Shrestha et al., 2010). In this study, after 7 days'

415   incubation, the sediment microcosm with the highest ammonium dosage had much

416   higher *pmoA* gene abundance than un-amended microcosm and other amended

417   microcosms with lower dosage, whereas no significant difference of *pmoA* gene

418   abundance was detected between un-amended microcosm and amended microcosms

419   (except for the treatment with the highest ammonium dosage). After 14 days'

420   incubation, the microcosm with the highest ammonium dosage also had much higher

421   DNA-based methanotrophic abundance than other amended microcosms. Hence, the

422   present study further provided the evidence that the addition of ammonium,

423   depending on dosage, could influence freshwater sediment DNA-based

424   methanotrophic abundance, which was in agreement with the result of two-way

425   ANOVA. Dianchi Lake had been suffering from eutrophication for over 30 years

426   (Huang et al., 2017). It could be assumed that methanotroph community in this lake

427   had been adapted to high in-situ ammonia concentration. As a result, only extremely

428   high dosage of ammonium could pose a significant impact on DNA-based

429   methanotrophic abundance.

430

431   At each time, the microcosm with no external ammonium addition had lower

432   abundance of *pmoA* transcripts than each amended microcosm. This suggested the

433   addition of ammonium could influence the transcription of *pmoA* gene. The

434   stimulation of *pmoA* transcription by the addition of ammonium could be attributed to

435   the competition between methane and ammonium for the binding site of pMMO

436   (Bédard and Knowles, 1989). This was also verified by the similar number of

437   transcripts in these amended microcosms after the considerable reduction of

438   ammonium. At days 1 and 14, the abundance of *pmoA* transcripts differed greatly in

439   different amended microcosms. This suggested that ammonium dosage could

440   influence the number of *pmoA* transcripts, which was consistent with the result of

441   two-way ANOVA.

442

443   *4.3. Effect of ammonium on DNA- and RNA-based* methanotrophic *community*

444   *compositions*

445   Several previous studies have investigated the influence of ammonium amendment on

446   soil methanotrophic community structure (Alam and Jia, 2012; Mohanty et al., 2006;

447   Shrestha et al., 2010), yet information about the influence of ammonium amendment

448   on freshwater methanotrophic community structure is still lacking. In this study,

449   immediately after ammonium addition (after 12-h incubation), the relative abundance

450   of Type I (especially Type Ia) methanotrophs transcripts increased, instead of Type II.

451   This coincided with the result reported in rice and forest soils (Mohanty et al., 2006).

452   This also suggested that a high level of ammonia favored the growth of Type I

453   methantrophs and they might play an important role in methane oxidation in

454   ammonia-rich lake. However, both DNA- and RNA-based T-RFLP profiles indicated

455   that the addition of ammonium lead to an increase in the ratio of Type II to Type I

456   methanotrophs in two weeks, which was contrary to the results observed in some

457   previous studies in soil ecosystems (Alam and Jia, 2012; Bodelier et al., 2000;

458   Mohanty et al., 2006). These previous studies found that Type I methanortrophs had a

Biogeosciences

Discussions

Open Access

EGU

459   numerical advantage over Type II at a high ammonia concentration. Our recent field

460   study suggested that that the abundance of Type II methanotrophs in sediment of

461   Dianchi Lake was closely correlated to the concentration of ammonia (Yang et al.,

462   2016). Therefore, the response of methanotrophs to ammonia might depend on the

463   type of ecosystem. In addition, the community compositions of *pmoA* genes and

464   transcripts could be divergent, and DNA-based and RNA-based methanotrophs could

465   show different responses to ammonium addition (Shrestha et al. 2010). In this study,

466   compared with *pmoA* gene, the community structure of *pmoA* transcripts was more

467   sensitive to external ammonium addition. This was in a consensus with the result of a

468   previous study on the effect of ammonium addition on methanotrophs in root and

469   rhizospheric soils (Shrestha et al. 2010).

470

471   **5.   Conclusions**

472   This was the first microcosm study on the influence of ammonium on freshwater lake

473   sediment methanotroph community. In freshwater lake sediment microcosm, methane

474   oxidation potential and methanotrophic community could be influenced by

475   ammonium amendment. Ammonia concentration had a significant impact on

476   methanotrophic abundance and diversity, but exerted no evident influence on

477   community structure. Compared with *pmoA* gene, transcripts were more sensitive to

478   external ammonium addition. Further works are necessary in order to elucidate the

479   influence of ammonium on methane oxidation in freshwater sediment.

480

Conflict of interest

The authors declare that they have no competing interests.

483

488

References

Alam, M., Jia, Z., 2012. Inhibition of methane oxidation by nitrogenous fertilizers in a

paddy soil. Front. Microbiol. 3, 246.

Bastviken, D., Cole, J., Pace, M., Tranvik, L., 2004. Methane emissions from lakes:

Dependence of lake characteristics, two regional assessments, and a global

estimate. Glob. Biogeochem. Cycle 18, GB4009.

Bastviken, D., Cole, J., Pace, M., de Bogert, M., 2008. Fates of methane from

different lake habitats: Connecting whole-lake budgets and CH_4 emissions. J.

Geophys. Res.-Biogeosci.113, G02024.

Bédard, C., Knowles, R., 1989. Physiology, biochemistry, and specific inhibitors of

CH_4, NH_4^+, and CO oxidation by methanotrophs and nitrifiers. Microbiol. Rev. 53,

68–84.

24

Biogeosciences
Discussions

Open Access

EGU

501   Bodelier, P.L.E., Roslev, P., Henckel, T., Frenzel, P., 2000. Stimulation by ammonium-

502   based fertilizers of methane oxidation in soil around rice roots. Nature 403, 421–

503   424.

504   Bodelier, P.L.E., Laanbroek, H.J., 2004. Nitrogen as a regulatory factor of methane

505   oxidation in soils and sediments. FEMS Microbiol. Ecol. 47, 265–277

506   Borjesson, G., Nohrstedt, H.O., 2000. Fast recovery of atmospheric methane

507   consumption in a Swedish forest soil after single-shot N-fertilization. For. Ecol.

508   Manage. 134, 83–88.

509   Borrel, G., Jezequel, D., Biderre-Petit, C., Morel-Desrosiers, N., Morel, J.P., Peyret,

510   P., Fonty, G., Lehours, A.C., 2011. Production and consumption of methane in

511   freshwater lake ecosystems. Res. Microbiol. 162, 832–847.

512   Bosse, U., Frenzel, P., Conrad, R., 1993. Inhibition of methane oxidation by

513   ammonium in the surface layer of a littoral sediment. FEMS Microbiol. Ecol. 13,

514   123–134.

515   Danilova, O.V., Suzina, N.E., Van De Kamp, J., Svenning, M.M., Bodrossy, L.,

516   Dedysh, S.N., 2016. A new cell morphotype among methane oxidizers, a spiral-

517   shaped obligately microaerophilic methanotroph from northern low-oxygen

518   environments. ISME J 10, 2734–2743.

519   Jang, I., Lee, S., Zoh, K.D., Kang, H., 2011. Methane concentrations and

520   methanotrophic community structure influence the response of soil methane

521   oxidation to nitrogen content in a temperate forest. Soil Biol. Biochem. 43, 620–

522   627.

523   Huang, C.C., Yao, L., Zhang, Y.L., Huang, T., Zhang, M.L., Zhu, A.X., Yang, H.,

524   2017. Spatial and temporal variation in autochthonous and allochthonous

525   contributors to increased organic carbon and nitrogen burial in a plateau lake. Sci.

526   Total Environ. 603, 390–400.

527   Kumar, S., Stecher, G., Tamura, K., 2016. MEGA7: Molecular evolutionary genetics

528   analysis version 7.0 for bigger datasets. Mol. Biol. Evol. 33, 1870–1874.

529   Letunic, I., Bork, P., 2016. Interactive tree of life (iTOL) v3, an online tool for the

530   display and annotation of phylogenetic and other trees. Nucleic Acids Res. 44,

531   W242–W245.

532   Liikanen, A., Martikainen, P.J., 2003. Effect of ammonium and oxygen on methane

533   and nitrous oxide fluxes across sediment–water interface in a eutrophic lake.

534   Chemosphere 52, 1287–1293.

535   Liu, Y., Zhang, J.X., Zhao, L., Li, Y.Z., Yang, Y.Y., Xie, S.G., 2015. Aerobic and

536   nitrite-dependent methane-oxidizing microorganisms in sediments of freshwater

537   lakes on the Yunnan Plateau. Appl. Microbiol. Biotechnol. 99, 2371–2381.

538   Mohanty, S.R., Bodelier, P.L., Floris, V., Conrad, R., 2006. Differential effects of

539   nitrogenous fertilizers on methane-consuming microbes in rice field and forest

540   soils. Appl. Environ. Microbiol. 72, 1346–1354.

Biogeosciences
Discussions

Open Access
EGU

541   Murase, J., Sugimoto, A., 2005. Inhibitory effect of light on methane oxidation in the

542   pelagic water column of a mesotrophic lake (Lake Biwa, Japan). Limnol.

543   Oceanogr. 50, 1339–1343.

544   Nold, S.C., Boschker, H.T.S., Pel, R., Laanbroek, H.J., 1999. Ammonium addition

545   inhibits 13C-methane incorporation into methanotroph membrane lipids in a

546   freshwater sediment. FEMS Microbiol. Ecol. 29, 81–89.

547   Nyerges, G., Stein, L.Y., 2009. Ammonia cometabolism and product inhibition vary

548   considerably among species of methanotrophic bacteria. FEMS Microbiol. Lett.

549   297, 131–136.

550   Oksanen. J, Blanchet, F.G., Friendly, M., Kindt, R., Legendre P., McGlinn, D.,

551   Minchin, P.R., O'Hara, R. B., Simpson G.L, Solymos, P., Stevens M.H.H.,

552   Szoecs, E., Wagner, H., 2018. Vegan, Community ecology package, version 2.4-

553   6, Available at, https,//CRAN.R-project.org/package=vegan.

554   Rudd, J.W.M., Hamiltion, R.D., 1975. Factors controlling rates of methane oxidation

555   and the distribution of the methane oxidizers in a small stratified lake. Arch.

556   Hydrobiol. 75, 522–538.

557   Rudd, J.W.M., Furutani, A., Flett, R.J., Hamilton, R.D., 1976. Factors controlling

558   methane oxidation in Shield Lakes: The role of nitrogen fixation and oxygen

559   concentration. Limnol Oceanogr, 21, 357–364.

560   Seghers, D., Top, E.M., Reheul, D., Bulcke, R., Boeckx, P., Verstraete, W., Siciliano,

561   S.D., 2003. Long-term effects of mineral versus organic fertilizers on activity

562   and structure of the methanotrophic community in agricultural soils. Environ.

563   Microbiol. 5, 867–877.

564 Shrestha, M., Shrestha, P.M., Frenzel, P., Conrad, R., 2010. Effect of nitrogen

565   fertilization on methane oxidation, abundance, community structure, and gene

566   expression of methanotrophs in the rice rhizosphere. ISME J 4, 1545–1556.

567 Veraart, A.J., Steenbergh, A.K., Ho, A., Kim, S.Y., Bodelier, P.L.E., 2015. Beyond

568   nitrogen: The importance of phosphorus for CH_4 oxidation in soils and

569   sediments. Geoderma 259, 337–346.

570 Yang, Y.Y., Zhao, Q., Cui, Y.H., Wang, Y.L., Xie, S.G., Liu, Y., 2016. Spatio-

571   temporal variation of sediment methanotrophic microorganisms in a large

572   eutrophic lake. Microb. Ecol. 71, 9–17.

573 Zhang, X., Kong, J.Y., Xia, F.F., Su, Y., He, R., 2014. Effects of ammonium on the

574   activity and community of methanotrophs in landfill biocover soils. Syst. Appl.

575   Microbiol. 37, 296–304.

576

577

578

579

580

581

582

583

Biogeosciences
Open Access
Discussions
EGU

584

585

586

587 **Table 1** Numbers of T-RFs and T-RF-based Shannon diversity. For sample name,

588 upper case letters refer to treatment while digits indicate sampling time.

Sample	DNA		RNA	
	T-RFs	Shannon	T-RFs	Shannon
A1	11	1.55	23	2.55
B1	11	1.55	23	2.23
C1	11	1.49	22	2.17
D1	11	1.27	14	1.70
E1	11	1.48	20	2.12
F1	12	1.66	25	2.55
A7	12	1.74	28	2.92
B7	12	1.80	32	3.09
C7	13	1.77	27	2.86
D7	12	1.79	18	2.46
E7	14	1.89	30	2.98
F7	13	1.70	24	2.70
A14	13	1.70	36	3.17
B14	12	1.79	38	3.09
C14	12	1.83	33	2.96
D14	12	1.87	34	3.08
E14	12	1.83	32	2.89
F14	12	1.79	20	2.18

589

590

591

592

593

594

595

596

597   **Fig. 1.** Change of methane oxidation potential in the microcosms with different

598   treatments. Error bar indicates standard deviation (*n*=3). Asterisk indicates the

599   significance between experiment group and control group (*P*< 0.05). 'ns' indicates no

600   significant difference among treatments at a given time.

601
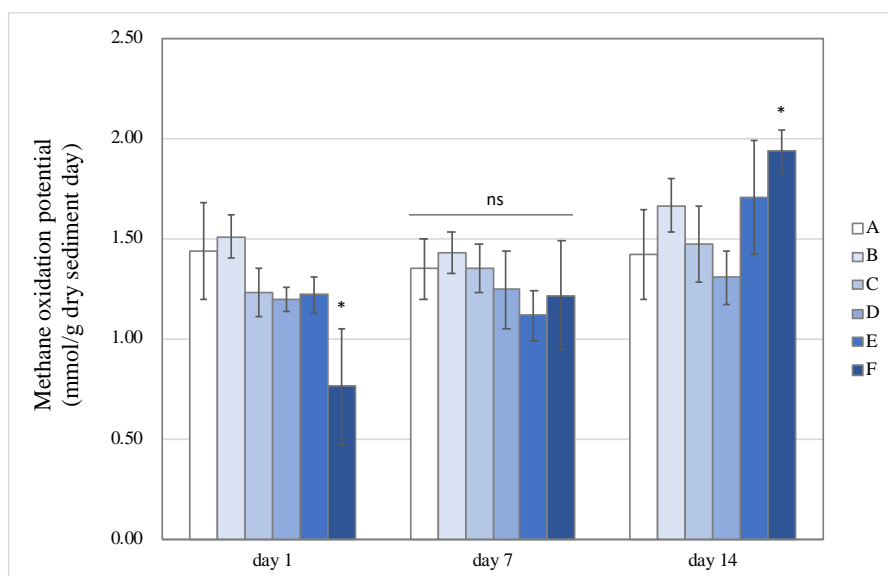
602
603
604
605
606
607
608
609
610
611
612
613

614   **Fig. 2.** Changes of *pmoA* gene (a) and transcript (b) abundance in the microcosms

615   with different treatments. Error bar indicates standard deviation (*n*=3). Asterisk

616   indicates the significance between experiment group and control group (*P*<0.05). 'ns'

617   indicates no significant difference among treatments at a given time.

618   **(a)**
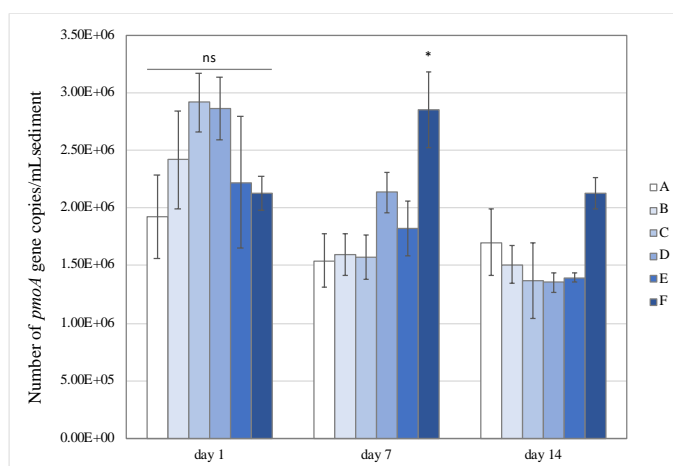
619

620

621   **(b)**
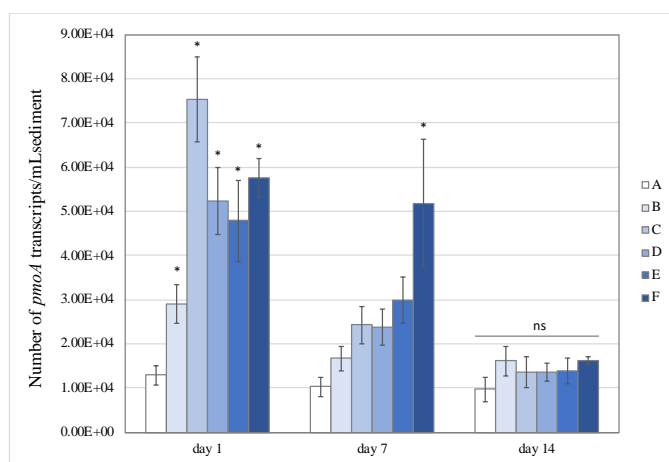
622

623

624 **Fig. 3.** Phylogenetic tree of obtained *pmoA* sequences and reference sequences from

625 the GenBank database. The predicted cut sites were shown after the accession

626 numbers of sequences. The dots at branches represent the support values from

627 bootstrap test. Branch support values of no less than 50 were dotted. The bar

628 represents 1% sequence divergence based on neighbor-joining algorithm.
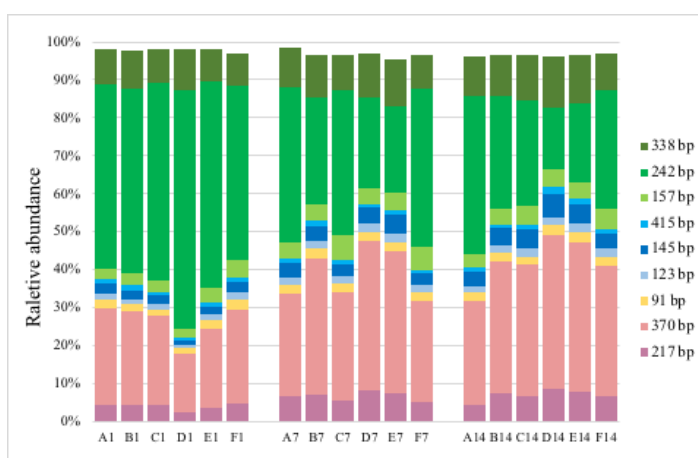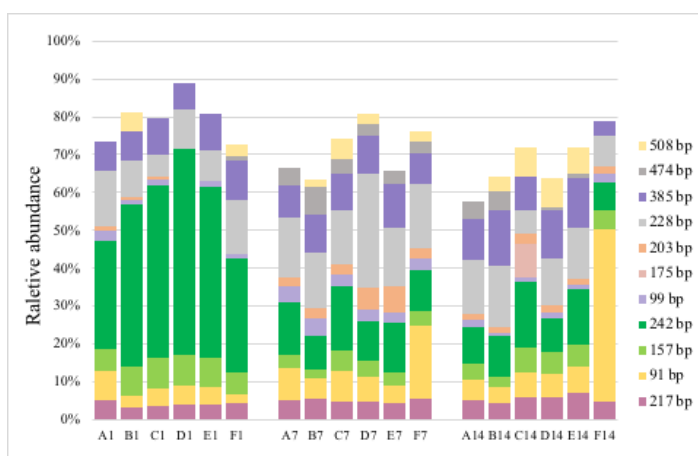
629
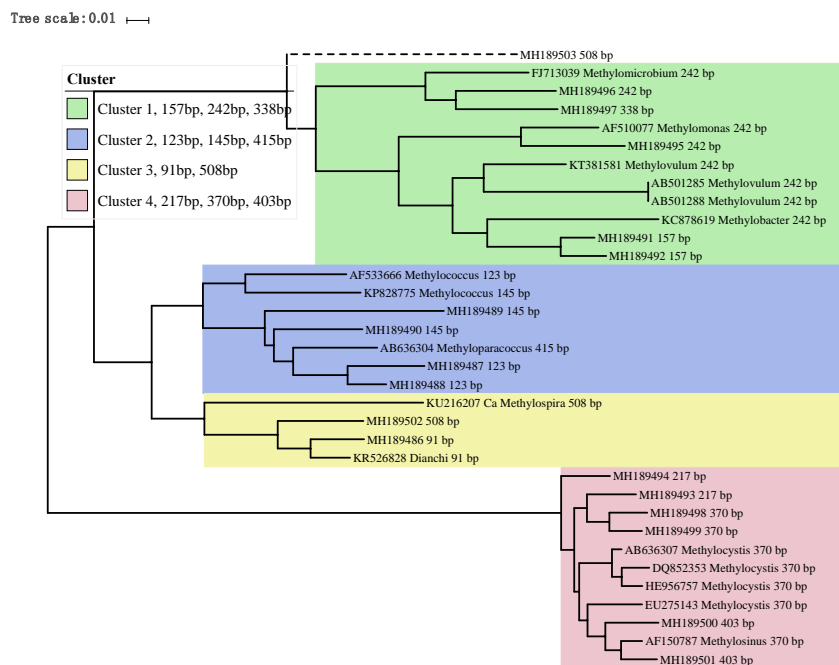
630
631
632
633
634
635
636
637
638

639

640

641 **Fig. 4.** T-RFLP profiles based on *pmoA* gene (a) and transcripts (b). For sample name,

642 upper case letters refer to treatment while digits indicate sampling time.
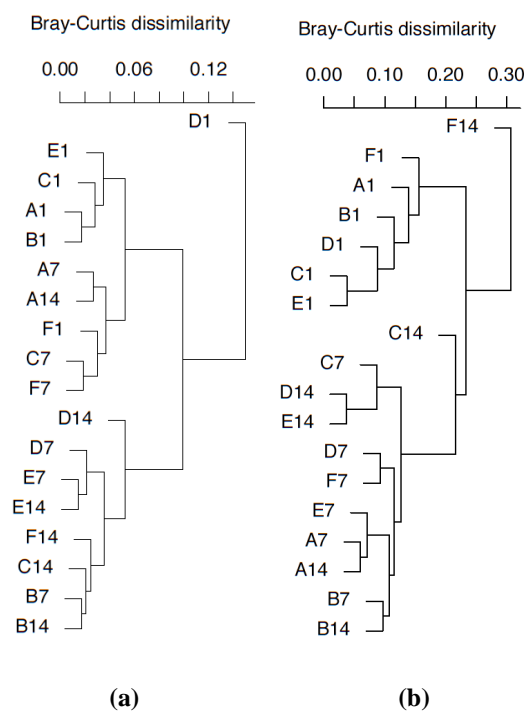
643 **(a)**

644
645

646 **(b)**

647
648
649
650
651
652

653 **Fig. 5.** *pmoA* gene (a) and transcripts (b)-based cluster diagrams of similarity values

654 for samples with different treatments. Dissimilarity levels are indicated above the

655 diagram. For sample name, upper case letters refer to treatment while digits indicate

656 sampling time.

657

658

659 **(a)** **(b)**

660

661

662

663

664